Star Mesogen-Jacketed Liquid Crystalline Polymers with Silsesquioxane Core: Synthesis and Characterization

Qiwei Pan, Longcheng Gao, Xiaofang Chen, Xinghe Fan,* and Qifeng Zhou*

Beijing National Laboratory for Molecular Sciences, Key Laboratory of Polymer Chemistry and Physics of Ministry of Education, College of Chemistry and Molecular Engineering, Peking University, Beijing 100871, China

Received January 25, 2007; Revised Manuscript Received May 8, 2007

ABSTRACT: To study how architecture affects the liquid crystalline behavior of mesogen-jacketed liquid crystalline polymers (MJLCPs), a series of eight-arm star poly{2,5-bis[(4-methoxyphenyl)oxycarbonyl]styrene} (PMPCS) were synthesized and carefully characterized. The star polymers were successfully synthesized by atom transfer radical polymerization (ATRP) with octakis(2-bromo-2-methylpropionoxypropyldimethylsiloxy)-octasilsesquioxane (OBPS) as initiator. Arms of the star polymers were released by destroying the silsesquioxane core with hydrofluoric acid, and the precise octafunctionality of the star polymers was confirmed by gel permeation chromatography equipped with a multiangle laser light scattering detector. DSC, one- and two-dimensional wide-angle X-ray diffraction, and polarized optical microscopy were used to study the molecular weight dependent phase behavior of the eight-arm star PMPCS. It was found that when $M_{n,star}^{GPC} < 4.48 \times 10^4$ g/mol, only amorphous state could be observed; when $M_{n,star}^{GPC} \geq 4.48 \times 10^4$ g/mol, Φ_{HN} phase developed. The eight-arm star PMPCS required less monomer units per arm to stabilize the liquid crystalline phase compared to the linear ones, and hexagonal packing of the cylinder-like linear arms developed in the eight-arm star PMPCS, although the linear arms were amorphous or just had nematic packing.

Introduction

Synthesis of polymers with well-defined architectures has got more and more attention these years due to the great development of the polymerization method.[1] Polymers with unique structures, such as star, brush, comb, and gradient, have been successfully prepared and utilized in many areas. Star polymer, which is a macromolecule having one branching point (core) and having arms with about the same molecular weight, is considered as the simplest model of branched polymers.[2] It exhibits unique properties both in solution[3] and in bulk.[4,5]

Star polymers containing functional arms like liquid crystalline polymers (LCPs),[6] bio-related polymers,[7] and electrooptical polymers[8] take advantage of both functionality and good processability, so they have generated great attention and excitement in the materials community. Pugh et al.[9−11] first reported the synthesis of well-defined three-arm and six-arm star side-chain liquid crystalline polymers (SCLCPs) via ATRP and studied their thermotropic behavior. They find that the starlike topology does not change the mesophase structure but lowers the phase transition temperature in comparison with the linear analogue. Kricheldorf et al.[12] synthesized four-arm star main-chain liquid crystalline polymers (MCLCPs) by condensation polymerization using a multifunctional core. Different from star SCLCPs, they find that the star MCLCPs have higher glass transition temperature and lower crystallinity. The results from Polk et al.[13] also show that four-arm starlike wholly aromatic polyester possesses low crystallinity due to the branched structure.

Since most of the mesophases formed by SCLCPs are caused by parallel alignment of mesogenic units in the polymers, topology of the polymers may not have great influence on the phase structure, which was proved by Pugh's work. However, if the mesophases are resulted from parallel packing of the rodlike polymer chains, the branched structures may dramatically affect the phase behavior, for the packing behavior could be favored or prohibited in different cases. Unfortunately, related reports on star polymers containing rodlike arms are quite rare.

Mesogen-jacketed liquid crystalline polymers (MJLCPs) have similar chemical structures with conventional SCLCPs, except that the mesogenic groups are laterally attached to the backbone through their center of gravity with short or no spacers.[14−17] Rigid side groups densely warping around the flexible main chain, so-called jacketed effect, makes the flexible backbones adopt a nearly extended conformation. Thus, the mesophase behaviors of MJLCPs are quite different from those of SCLCPs. It is the whole semirigid polymer chains, instead of the mesogenic side chains, that pack parallelly to each other to form supramolecular columnar phases. On the other hand, because monomers of MJLCPs are derivatives of styrene, living free radical polymerizations of them can be performed. Linear homopolymers[18,19] as well as rod−coil block copolymers[20,21] based on MJLCPs have been produced by ATRP, and the very first three-arm star block MJLCP[22] was obtained by the nitroxide-mediated approach, so it is possible to synthesize well-defined star homo-MJLCPs if a proper synthetic method is applied. The facile synthesis of star MJLCPs makes it possible to study how architecture affects the liquid crystalline properties of star LCPs which have arms with rodlike conformations.

There are two essential methods to synthesize well-defined star polymers: "arm-first" method and "core-first" method. The former one is linking the linear chains to a central core, while the latter one is growing the branches from a multifunctional core.[23] Since the "arm-first" method always leads to ill-defined star polymers with a distribution of arm numbers, the "core-first" method is more popular in preparation of star polymers with precise arm number and arm length, especially after the

* To whom correspondence should be addressed. E-mail: fanxh@pku.edu.cn; qfzhou@pku.edu.cn.

10.1021/ma070207d CCC: $37.00
Published on Web 06/16/2007

Scheme 1. Synthesis of Eight-Arm Star Poly{2,5-bis[(4-methoxyphenyl)oxycarbonyl]styrene} by Atom Transfer Radical Polymerization Using Octafunctional Silsesquioxane as Initiator[a]

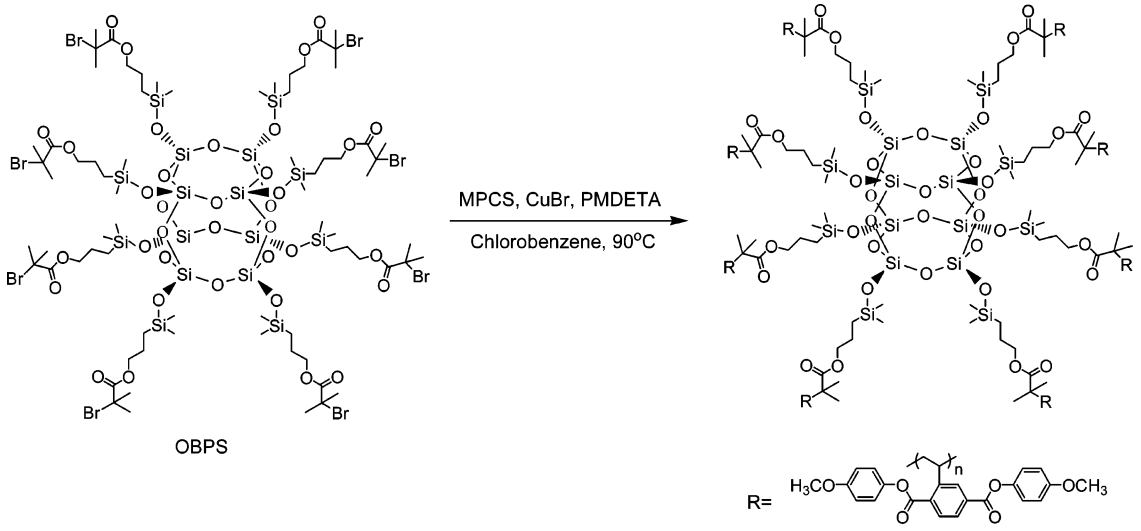

[a] MPCS = 2,5-bis[(4-methoxyphenyl)oxycarbonyl]styrene; PMDETA = *N*,*N*,*N*′,*N*′,*N*′′-pentamethyldiethylenetriamine.

appearance of atom transfer radical polymerization (ATRP).[24] Different multifunctional initiators, such as calixarene, dendritic multifunctional initiators, and octafunctional silsesquioxanes, have been used to prepare star polystyrene, polyacrylate, and polymethacrylate with high arm number (>4).[25−37] The problem with most of the cases is that polymerization has to stop at low monomer conversion to prevent coupling termination. Hence, how to synthesize well-defined star polymers with high arm number in high monomer conversion is still challenging.

Among the multifunctional initiators mentioned above, octakis(2-bromo-2-methylpropionoxypropyldimethylsiloxy)-octasilsesquioxane (OBPS)[32] is very attractive because the tertiary bromoester group has high initiation efficiency during ATRP. Meanwhile, the silsesquioxane core can be destroyed easily with hydrofluoric acid, which provides a facile way to study the characters of the arms. 2,5-Bis[(4-methoxyphenyl)-oxycarbonyl]styrene (MPCS) is a typical mesogen-jacketed liquid crystalline monomer, and the phase behavior of the resulting polymer has be investigated in detail.[38] Therefore, OBPS was selected as an initiator for ATRP of MPCS to prepare eight-arm star MJLCPs in this work. ATRP was under good control, even when the monomer conversion is as high as 80%. Well-defined eight-arm star PMPCS with high molecular weight were synthesized. Octafunctionality of the star polymers was fully characterized, and the dependence of phase transition and structure on the molecular weight was also investigated.

Experiment

Materials. Octakis(dimethylsilyloxy)silsesquioxane ($Q_8M_8^H$, 97%, Aldrich), platinum(0)−1,3-divinyl-1,1,3,3-tetramethyldisiloxane complex (Pt(dvs), solution in xylene, Aldrich), 2-bromo-2-methylpropanoyl bromide (99%, Acros), and *N*,*N*,*N*′,*N*′,*N*′′-pentamethyldiethylenetriamine (PMDETA, 99%, Aldrich) were used as received. Toluene was distilled from Na/benzophenone under N_2. Chlorobenzene was purified by washing with concentrated sulfuric acid to remove thiophene, followed by washing with water, then dried, and distilled. Cuprous bromide (CuBr) was synthesized from $CuBr_2$ and purified by stirring in glacial acetic acid, then filtering and washing with methanol, and dried under vacuum. Other reagents were commercially available and used without purification. 2,5-Bis[(4-methoxyphenyl)oxycarbonyl]styrene (MPCS) was synthesized according to the literature.[39]

Synthesis of Octafunctional Initiator: Octakis(2-bromo-2-methylpropionoxypropyldimethylsiloxy)octasilsesquioxane (OBPS). The initiator was synthesized according to the route described by Laine et al.[32] The yellowish wax product obtained was further purified by silica gel column chromatography with petroleum ether and ethyl acetate as eluent to remove the high molecular weight portion. Light yellow solid was obtained with yield of 51%. ^{1}H NMR (400 MHz, $CDCl_3$, $CHCl_3$ ref): 4.14 (t, 16H,CH_2−O), 1.94 (s, 48H, (CH_3)$_2$−C(Br)(C═O)), 1.73 (p, 16H, CH_2−CH_2−CH_2), 0.66 (t, 16H, CH_2−Si), 0.18 (s, 48H, (CH_3)$_2$−Si). ^{13}C NMR (100 MHz, $CDCl_3$, $CHCl_3$ ref): 171.6 (*C*═O), 68.2 (*C*H_2−O), 55.9 (*C*−C═O), 30.8 ((*C*H_3)$_2$C(Br)(C═O)−), 22.1 (CH_2−*C*H_2−CH_2), 13.4 (*C*H_2−Si), −0.3 ((*C*H_3)$_2$-Si). ^{29}Si NMR (119.2 MHz, $CHCl_3$): 12.0 (O*Si*(CH_3)$_2$CH_2), −109.8 (*Si*O$_4$). Anal. Calcd for $C_{64}H_{144}O_{36}Si_{16}Br_8$: C 32.33, H 5.43. Found: C 32.64, H 5.49. GPC analysis: M_n = 2205, PDI = 1.01.

Synthesis of Eight-Arm Star PMPCS. OBPS, MPCS, CuBr, PMDETA, and chlorobenzene, the amounts of which were determined by the designed molecular weight, were placed in a dry glass tube. After three freeze−pump−thaw cycles, the tube was sealed under vacuum and placed into an oil bath thermostated at 90 °C for a specific time. Then it was broken after the polymerization was terminated by putting it into an ice/water mixture. The crude product was diluted with THF and passed through a basic alumina column to remove the copper complex. The polymers were precipitated into methanol three times before being used. The white mass obtained was vacuum-dried and used. Monomer conversion was measured by gravimetry.

Release of Arms. About 20 mg of star PMPCS was put into a plastic tube and dissolved in THF. Five drops of hydrofluoric acid were added to the tube, and then the tube was sealed. The solution was stirred at room temperature for 3−4 days to make sure that all cores were destroyed, and the crude product was precipitated in methanol and dried.

Equipment and Experiments. ^{1}H NMR and ^{13}C NMR were recorded on a Bruker ARX400 MHz spectrometer. ^{29}Si NMR spectra were recorded on JEOL ECA-600 MHz spectrometer operated at 119.2 MHz. Elemental analyses were performed on an Elementar Vario EL instrument. Gel permeation chromatographic (GPC) measurements were performed with a Waters 2410 refractive index detector at 35 °C, and THF was used as the eluent at the flow rate of 1.0 mL/min. Three Waters Styragel columns with 10 μm bead size were connected in series. Their effective molecular weight ranges were 100−10 000 for Styragel HT2, 500−30 000 for Styragel HT3, and 5000−600 000 for Styragel HT4. The pore sizes are 50, 100, and 1000 nm for Styragels HT2, HT3, and HT4, respectively. All GPC data were calibrated with linear polystyrene standards.

Absolute molecular weight was determined by GPC with a multiangle laser light scattering detector (GPC/MALLS) at 35 °C using THF as solvent (1.0 mL/min), a set of 50, 100, and 1000 nm Styragels columns, and a Wyatt Technology DAWN HELEOS 18 angle (from 15° to 165°) light scattering detector equipped with a Ga−As laser (658 nm, 40 mW), with the concentration at each elution volume determined using a Wyatt Optilab Rex interferometeric differential refractometer (658 nm). The molecular weight data were calculated using Astra 5.1.6.0 software (Wyatt Technology). Refractive index (RI) increments (d*n*/d*c*, using 1.0, 2.0, 3.0, 4.0, and 5.0 mg/mL) were measured off-line in THF (distilled from CaH_2 and filtered through a 0.45 μm PTFE filter; d*n*/d*c* = 0.172 mL/g) at room temperature at 658 nm using the Optilab Rex interferometeric refractometer calibrated with aqueous NaCl. All samples were dissolved overnight and filtered through a 0.45 μm PTFE filter.

Thermogravimetric analysis (TGA) was performed on a TA Q600 instrument at a heating rate of 10 °C/min in nitrogen atmosphere. The thermal transitions of the polymers were detected using Perkin-Elmer Pyris I DSC with a mechanical refrigerator. Samples with a typical mass of 3−7 mg were encapsulated in sealed aluminum pans. The samples were first heated to 250 °C and then cooled to −10 °C at 10 °C/min. This was followed by a second heating scan.

Polarized optical microscopy (POM) was conducted on a Leitz Laborlux 12 microscope coupled with a Leitz 350 hot stage.

1D-WAXD powder experiments were performed on a Philips X'Pert Pro diffractometer with a 3 kW ceramic tube as the X-ray source (Cu Kα) and an X'celerator detector. The sample stage was set horizontally. The reflection peak positions were calibrated with silver behenate (2θ < 10°) and silicon powder (2θ > 15°). Background scattering was recorded and subtracted from the sample patterns. To study the structure evolutions as a function of temperature, a temperature control unit (Paar Physica TCU 100) was conjunct with the diffractometer. The heating and cooling rates of the experiments were 10 °C/min.

2D-WAXD fiber patterns were obtained from a Bruker D8 Discover diffractometer with GADDS as a 2D detector. Silicon powder and silver behenate were used as standards again. Samples were mounted on the sample stage, and the point-focused X-ray beam was aligned both perpendicular and parallel to the mechanical shearing direction. The 2D diffraction patterns were recorded in a transmission mode at room temperature. The oriented films were prepared by mechanically shearing of the samples at LC temperature.

Results and Discussion

Preparation of Eight-Arm Star MJLCPs. To obtain well-defined star polymers with high arm number (>4) by the core-first method, it is important to choose suitable multifunctional initiator that can efficiently initiate the polymerization of the chosen monomers. Octakis(2-bromo-2-methylpropionoxypropyldimethylsiloxy)octasilsesquioxane (OBPS) is proved to be an active initiator for ATRP of methyl metharylate.[32] On the other hand, 2,5-bis[(4-methoxyphenyl)oxycarbonyl]styrene (MPCS) is compatible with ATRP. Well-defined block copolymers, such as PDMS-*b*-PMPCS[40] and PCL-*b*-PMPCS,[41] have been synthesized by ATRP using 2-bromoisobutyrates as initiator and CuBr/PMDETA as catalyst complex. Therefore, eight-arm star PMPCS was synthesized via ATRP, using OBPS as initiator, CuBr as catalyst, and PMDETA as ligand in this work (see Scheme 1).

Intermolecular coupling of star polymers happens easily when concentration of the stars exceeds their critical overlapping concentration C^*,[25] so the concentration of monomer remains low in our polymerization. A kinetic study of the polymerization of MPCS was conducted with OBPS in chlorobenzene at 90 °C. As illustrated in Figure 1, the linear relationship between $\ln([M]_0/[M])$ and time indicates that the concentration of radicals

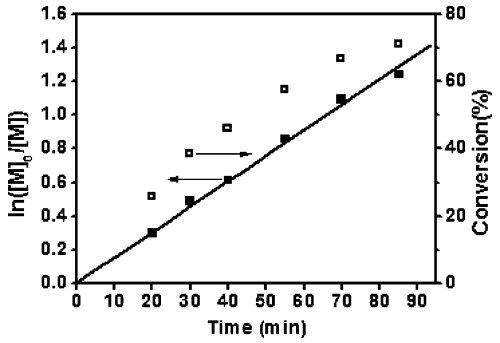

Figure 1. Kinetic plots of time dependence of monomer conversion and $\ln([M]_0/[M])$. Conditions: $[MPCS]_0$:$[OBPS]_0$:[CuBr/PMDETA] = 320:1:1, $[MPCS]_0$ = 0.5 mol/L, in chlorobenzene, at 90 °C.

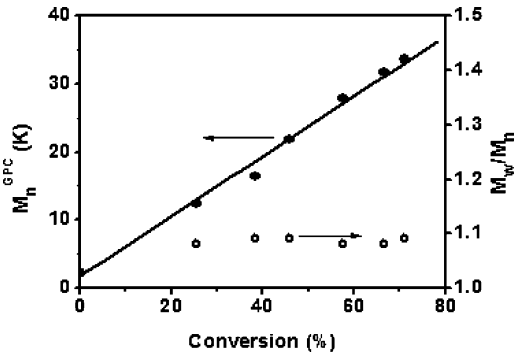

Figure 2. Dependence of molecular weight and molecular weight distribution by gel permeation chromatography on conversion of 2,5-bis[(4-methoxyphenyl)oxycarbonyl]styrene.

is constant during the polymerization and that the polymerization is first order with respect to the concentration of monomer. The molecular weight increases linearly with the monomer conversion, and the polydispersity of the star polymers remains low (see Figure 2). The GPC traces for star polymers are monomodal and symmetrically narrow when the monomer conversion is up to 71%. These results confirm that molecular weight controllable well-defined eight-arm star PMPCS can be obtained by the designed polymerization parameter.

Eight-arm star PMPCS with high molecular weight and narrow polydispersity can be prepared by increasing the ratio of $[M]_0/[I]_0$. Well-controlled ATRP was still achieved, and results are listed in Table 1. The absolute molecular weights detected by multiangle laser light scattering coupled with GPC line (MALLS/GPC) are close to the theoretical ones, indicating high initiation efficiency and few side reactions during polymerization. Star PMPCS with molecular weight up to 50.20×10^4 g/mol is obtained. However, the molecular weight determined by linear polystyrene standards is much underestimated. That is because the hydrodynamic radius of a star macromolecule is smaller than that of a linear one with the same molecular weight.[30,36] The polydispersity of all polymers is remarkably low.

When intermolecular coupling occurs during the polymerization, star polymers with much higher molecular weight are formed, but they cannot be detected by GPC line with a RI detector effectively if their content is low.[25] Laser light scattering is very sensitive to the high molecular weight portion, so MALLS/GPC is a reliable technique to detect star−star coupling. The monomodal and symmetrically narrow eluograms (MALLS/GPC) of the eight-arm star PMPCS in Table 1 illustrate that intermolecular coupling does not occur when the conversion is as high as 80% (Figure 3a).

Table 1. Results of Polymerization of 2,5-Bis[(4-methoxyphenyl)oxycarbonyl]styrene, Using Octafunctional Silsesquioxane as Initiator at Different $[M]_0/[I]_0$ Ratios

sample	$[M]_0/[I]_0$	$[M]_0$ (mol/L)	conv (%)	M_n[a] ($\times 10^4$, GPC)	M_n ($\times 10^4$, LLS)	M_{theo}[b] ($\times 10^4$)	PDI[a]	$M_{n,arms}$ ($\times 10^4$, LLS)	PDI[a] (arms)	F[c]
1	640	1.0	57.9	4.97	15.65	15.23	1.09	1.96	1.13	8.0
2	1040	0.8	47.2	6.45	20.09	18.59	1.07	2.46	1.12	7.6
3	1040	0.8	82.0	10.12	31.21	31.48	1.09	3.83	1.11	8.1
4	2000	1.0	60.8	16.36	50.20	49.30	1.07	6.73	1.12	7.5

[a] Calibrated by linear PS standards. [b] $M_{theo} = M_{MPCS} \times ([M]_0/[I]_0) \times$ conversion $+ M_{OBPS}$. [c] Arm number of each star, $F = M_n(LLS)/M_{n,arm}(LLS)$.

Star−star coupling is difficult to avoid in ATRP with multifunctional (>4) initiator.[25,26,32,35] Polymerization must be stopped at low monomer conversion to prepare well-defined star polymers. Therefore, it is interesting that the polymerization parameter designed here can lead to such well-controlled ATRP. There are two possible reasons for this. First, monomers of MJLCPs are very bulky; they have low coupling termination rate,[42] so termination cannot occur easily during polymerization. Second, all the polymerization was performed in low monomer concentration and low initiator concentration (less than 1.0 mol/L, Table 1), so ATRP without star−star coupling was achieved.

Characterization of Functionality. There are two methods to determine whether each of the alkyl halide fragments of the initiators is participating in the ATRP process. One is to characterize the individual arms obtained by cleaving the core of the star polymers.[25−27] Another is the kinetic approach proposed by Matyjaszewski et al.[36] For the eight-arm star PMPCS with a silsesquioxane core, the arms can be easily released by destroying the core with hydrofluoric acid, so the first method was preferred. The star PMPCS were treated with hydrofluoric acid for several days to make sure that all the silsesquioxane cores were destroyed. Functionality of the star PMPCS is obtained by comparing the molecular weight of the star polymers with those of their corresponding arms. It is close to eight (Table 1), confirming the well-defined star structure. (The functionality of some samples is not exactly eight due to some experimental errors.)

Coupling between two arms of one star is another kind of coupling termination. Different from intermolecular coupling, it cannot be detected by GPC of the star polymers, owing to its insignificant effect on the molecular weight of the star polymers. However, GPC curves of the arms will become asymmetric. GPC traces of the linear PMPCS obtained after destruction of the silsesquioxane core are monomodal and symmetry (Figure 3b), indicating negligible intramolecular coupling during polymerization.

On the basis of the above results, well-defined eight-arm star PMPCS can be successfully synthesized by ATRP of MPCS using OBPS as initiator, in the presence of CuBr/PMDETA. To study the liquid crystalline behavior of the eight-arm star MJLCPs, twelve samples with molecular weight from 0.63×10^4 to 15.76×10^4 g/mol (calculated by linear PS standards) and low polydispersity (Table 2) were synthesized. The molecular weight and polydispersity of their arms were also shown.

Thermal Behavior. The eight-arm star PMPCS has high thermal stability. Temperature of 5% weight loss is about 380 °C when the molecular weight exceeds 1.0×10^4 g/mol. Differential scanning calorimetry (DSC) was used to study the thermal transition of these samples. Only glass transitions can be observed in the DSC curves of all these star PMPCS samples during the first cooling and subsequent heating scans between −10 and 250 °C. The temperature of glass transition (T_g) was determined by second heating DSC thermal diagrams since the previous thermal histories of the samples were erased. Results are shown in Figure 4. T_g increases with increasing $M_{n,star}^{GPC}$ and reaches a plateau of 116 °C when $M_{n,star}^{GPC}$ exceeds 3.82×10^4 g/mol. When $M_{n,star}^{GPC}$ is lower than this value, T_g of the star polymers is lower than those of their linear analogues with the same molecular weight.

1D Wide-Angle X-ray Diffraction. 1D WAXD experiments were carried out to examine whether ordered structure developed in the as-cast samples during first heating. It is found that the phase structural development of these eight-arm star PMPCS samples is strongly molecular weight dependent. Two molecular weight regimes can be identified: the high molecular weight regime with $M_{n,star}^{GPC}$ reaching or exceeding 4.48×10^4 g/mol and low molecular weight regime with $M_{n,star}^{GPC}$ lower than 4.48

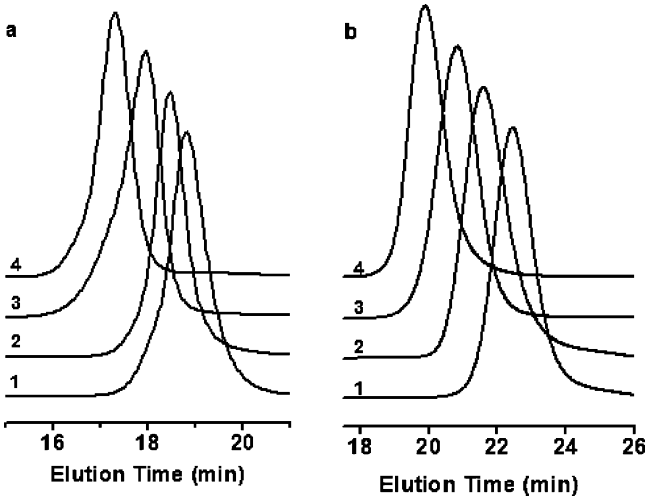

Figure 3. Gel permeation chromatographic traces of eight-arm star poly{2,5-bis[(4-methoxyphenyl)oxycarbonyl]styrene} (multiangle laser light scattering detector, a) and their corresponding arms (refractive index detector, b) in Table 1.

Table 2. Molecular Weight, Molecular Weight Distribution, and Phase Structure of Eight-Arm Star Poly{2,5-bis[(4-methoxyphenyl)oxycarbonyl]styrene} and Their Corresponding Arms

	stars			arms		
sample	$M_{n,star}^{GPC}$ [a] ($\times 10^4$)	PDI	LC[b]	$M_{n,arm}^{GPC}$ [a] ($\times 10^4$)	PDI	LC[c]
S-1	0.63	1.06	A	0.21	1.06	A
S-2	1.22	1.07	A	0.27	1.07	A
S-3	2.61	1.07	A	0.39	1.10	A
S-4	3.82	1.07	A	0.63	1.11	A
S-5	4.48	1.08	Φ_{HN}	0.74	1.08	A
S-6	4.97	1.09	Φ_{HN}	0.85	1.10	A
S-7	5.69	1.08	Φ_{HN}	0.96	1.12	A
S-8	6.45	1.07	Φ_{HN}	1.06	1.12	Φ_N
S-9	8.95	1.08	Φ_{HN}	1.49	1.08	Φ_N
S-10	10.12	1.09	Φ_{HN}	1.70	1.11	Φ_{HN}
S-11	11.39	1.07	Φ_{HN}	1.97	1.09	Φ_{HN}
S-12	15.76	1.10	Φ_{HN}	3.09	1.12	Φ_{HN}

[a] Calibrated by linear PS standards. [b] Phase structure of the eight-arm star PMPCS samples."A" represents "amorphous". [c] Results reported by Ye et al.[38] and confirmed again by polarized optical microscopy observation in our work.

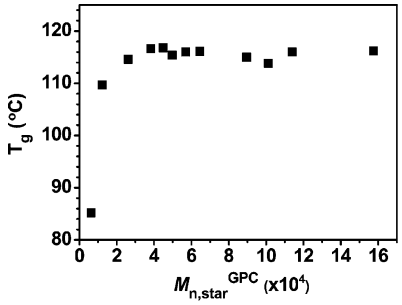

Figure 4. Molecular weight dependence of glass transition temperature of eight-arm star poly{2,5-bis[(4-methoxyphenyl)oxycarbonyl]styrene}.

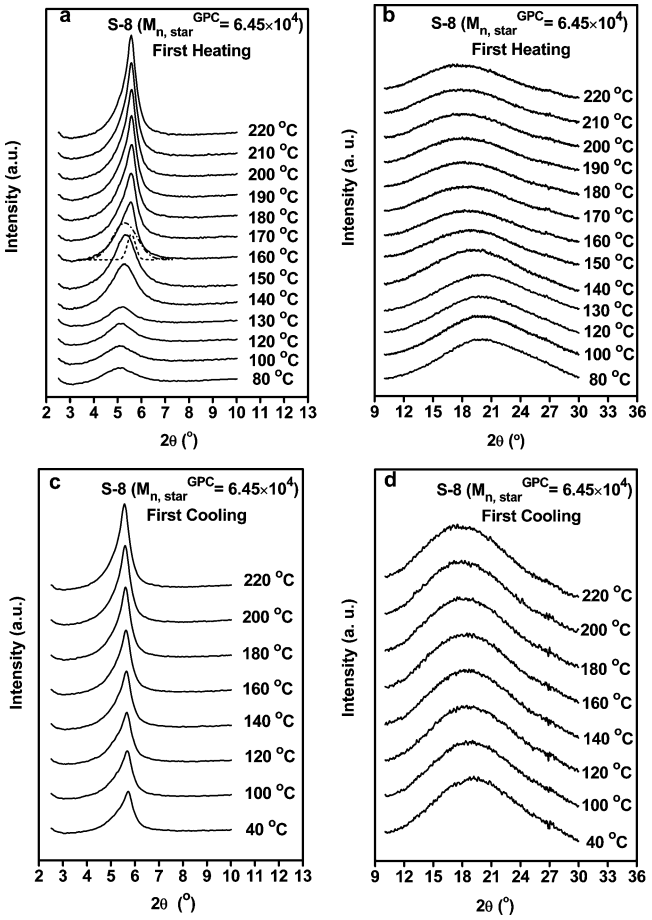

Figure 5. Set of one-dimensional wide-angle X-ray diffraction (WAXD) powder patterns in low 2θ angle region (a) and high 2θ angle region (b) of S-8 obtained during the first heating of the as-cast film. The corresponding first cooling WAXD powder patterns in both low and high 2θ angle region are shown in (c) and (d). The deconvolution of the reflection peak from the scattering halo in the low 2θ angle region during the first heating is shown by dashed curves at 160 °C in (a).

× 10^4 g/mol. S-8 ($M_{n,star}^{GPC}$ = 6.45 × 10^4 g/mol, $M_{n,arm}^{GPC}$ = 1.06 × 10^4 g/mol) and S-4 ($M_{n,star}^{GPC}$ = 3.82 × 10^4 g/mol, $M_{n,arm}^{GPC}$ = 0.63 × 10^4 g/mol) were used as representatives for these two molecular weight regimes.

Parts a and b of Figure 5 show the 1D WAXD patterns of the as-cast S-8 sample obtained during the first heating in both low 2θ (2.5°−10°) and high 2θ (10°−30°) angle region. In Figure 5a, a low angle scattering halo is observed when temperature is below 140 °C, and it dramatically increases its intensity and shifts to higher 2θ angle at 140 °C. Upon heating, the scattering halo becomes asymmetric and can be deconvoluted into one broad halo and a narrow reflection peak with centers at 2θ = 5.3° (d spacing of 1.66 nm) and 2θ = 5.6° (d spacing of 1.58 nm) separately (the dashed curves in Figure 5a). The positions of scattering halo and reflection peak are precisely decided by two Gaussian functions. Further heating the sample leads to increase of the reflection peak intensity, and the peak position slightly shifts to lower 2θ angle. In Figure 5b, only a high 2θ angle scattering halo can be observed, and its shape remains during the first heating. With increased temperature, the center of the scattering halo suddenly jumps to lower 2θ angle at 140 °C. This sudden shift of the scattering halo corresponds to the formation of ordered structure in nanometer length scale in Figure 5a. Above 140 °C, a slightly and continuously shift of the center of the scattering halo to lower 2θ angle is observed due to thermal expansion.

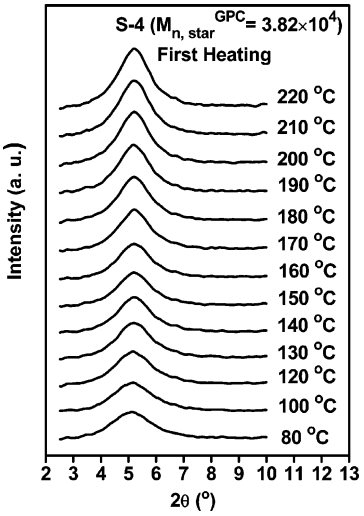

Figure 6. Set of one-dimensional wide-angle X-ray diffraction powder patterns in low 2θ angle region of S-4 obtained during the first heating of the as-cast film.

Cooling 1D WAXD experiment of the sample S-8 was carried out after first heating to 220 °C, as shown in parts c and d of Figure 5 for low and high 2θ angle regions, respectively. In the low 2θ angle region, the reflection peak at about 5.6° shifts continuously and slightly to higher 2θ angle, and its intensity decreases with decreasing temperature due to reduction of the periodic electron density contrast generating this reflection. In the high 2θ angle region, no sudden shift can be detected as observed in Figure 5b, and the broad scattering halo shifted continuously and slightly to a higher 2θ angle.

For the as-cast S-4 sample, 1D WAXD patterns in Figure 6 show that only a broad scattering halo can be observed for the entire temperature region. Upon raising temperature, the intensity of the scattering halo increases and keeps its shape. The center of the scattering halo shifts to a higher 2θ angle with increased temperature. It means that no ordered structure in nanometer length scale develops in this sample during heating.

In conclusion, all the as-cast samples are amorphous. But for eight-arm star PMPCS with $M_{n,star}^{GPC} \geq 4.48 \times 10^4$ g/mol, ordered structure on nanoscale develops in the first heating when the temperature is above the glass transition temperature. Meanwhile, this ordered structure remains after first heating.

Silsesquioxanes with alkyl groups attached on the eight corners are crystals with hexagonal cells.[43,44] When they are incorporated to the polymer matrix, crystallization of silsesquioxanes still happens,[45−48] even when the content of silsesquioxanes is as low as 1%. However, during the 1D-WAXD experiments of all eight-arm star PMPCS samples, no reflection peaks corresponding to the crystallization of silsesquioxanes can be detected, indicating that the silsesquioxanes are well-

dispersed in the PMPCS matrix and no aggregation occurs. Therefore, the silsesquioxane core just acts as a linking point in the eight-arm star PMPCS system and does not have a great effect on the liquid crystalline phase structure as it does in the low molecular weight liquid crystals system[49−51] due to the aggregation of silsesquioxanes.

Phase Identification of Eight-Arm Star PMPCS. 1D WAXD patterns lack dimensionality, so 2D wide-angle X-ray experiments were performed to identify the phase structures of the oriented eight-arm star PMPCS samples. Ye et al.[38] have reported detailed phase structure study on linear PMPCS. They find that the PMPCS backbone and its laterally attached mesogenic groups cooperatively assemble into cylindrical shape. When the molecular weight is higher than 1.60×10^4 g/mol, hexagonal lateral packing of the cylinders (lacked long-rang order) exists and named as Φ_{HN} phase. When the molecular weight is lower than 1.60×10^4 g/mol but higher than 1.00×10^4 g/mol, Φ_N phase is formed. Phase structure of the eight-arm star PMPCS was studied by the same method in this work.

Parts a and b of Figure 7 are 2D WAXD fiber patterns at room temperature of S-8. When the X-ray incident beam is perpendicular to the fiber axis and the fiber axis is parallel to the meridian direction (Figure 7a), a pair of strong diffraction arcs appear on the equator at $2\theta = 5.8°$ (d spacing of 1.52 nm), indicating that ordered structure has developed along the direction perpendicular to the fiber axis on nanometer scale. The scattering halo with broad azimuthal distribution in the high 2θ angle region on the meridian reveals that only short-range order exists along the fiber direction. No higher order diffractions can be detected on the equators even after a prolonged exposure time. When the X-ray incident beam is parallel to the fiber axis (Figure 7b), six diffraction arcs were located at $2\theta = 5.8°$ (d spacing of 1.52 nm). The corresponding azimuthal intensity profile showed in Figure 7c exhibits six maxima with an angle of 60° between the two adjacent diffraction maxima although the intensity is nonsymmetric due to imperfection of sample orientation during the experiment. Therefore, the liquid crystalline phase of S-8 should be hexatic columnar nematic (Φ_{HN}) phase. A hexagonal packing of the cylinders with each cylinder having an average diameter of 1.76 nm develops along the direction perpendicular to the fiber axis. However, this hexagonal packing lacks long-range order. Similar results are found for other eight-arm star PMPCS samples with $M_{n,star}^{GPC} \geq 4.48 \times 10^4$ g/mol.

Polarized optical microscopy (POM) was also used to study the liquid crystalline phase behavior of the star polymers. The POM image of S-8 is shown in Figure 8. It exhibits star-shaped texture, which is characteristic feature of Φ_{HN} phase in both linear PMPCS homopolymers[38] and MPCS-*co*-BCS random copolymers.[52] For samples with low M_n^{GPC}, no birefringence can be observed under POM in the temperature region studied irrespective of any thermal treatment (including heating, cooling, and isothermal conditions).

On the basis of the above results, molecular weight dependent phase behavior of the eight-arm star PMPCS was concluded in Table 2. Two regions can be identified: amorphous region where $M_{n,star}^{GPC}$ is lower than 4.48×10^4 g/mol ($M_{n,arm}^{GPC} = 0.74 \times 10^4$ g/mol) and Φ_{HN} phase region where $M_{n,star}^{GPC}$ reaches or exceeds 4.48×10^4 g/mol. Compared to linear PMPCS, the eight-arm star PMPCS requires fewer monomer units per arm to stabilize the liquid crystalline phase. The critical M_n^{GPC} for each arm is 0.74×10^4 g/mol in the star polymers, while it is 1.00×10^4 g/mol for linear PMPCS.[38] Furthermore, the starlike architecture of the macromolecules was found to affect the

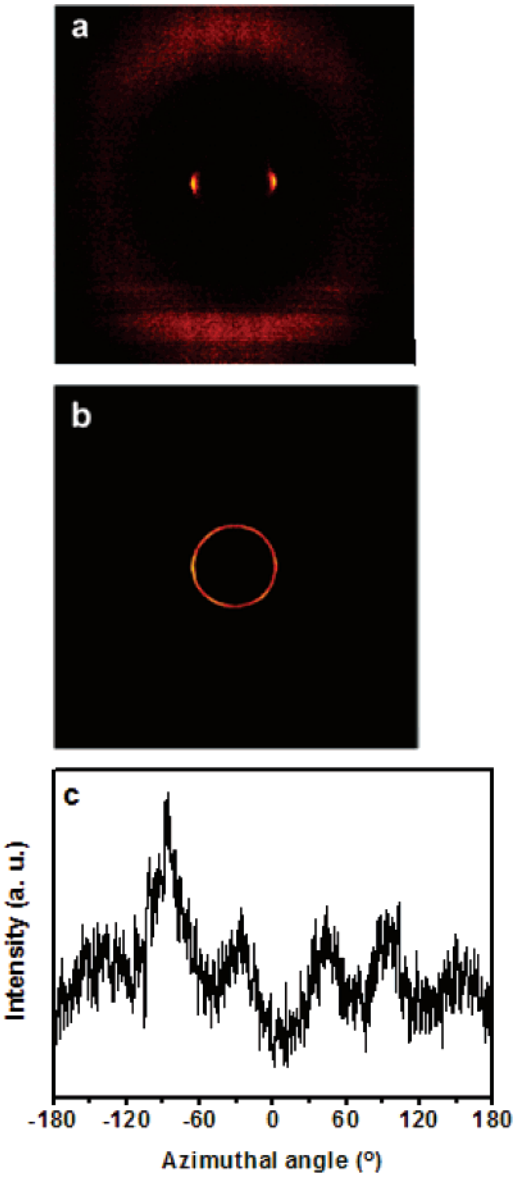

Figure 7. Two-dimensional wide-angle X-ray diffraction fiber patterns of S-8 detected at room temperature. The X-ray incident beam is perpendicular to the fiber axis (the meridian direction) (a) and parallel to the fiber direction (b). The azimuthal scanning data of the low 2θ angle diffraction in (b) is shown in (c).

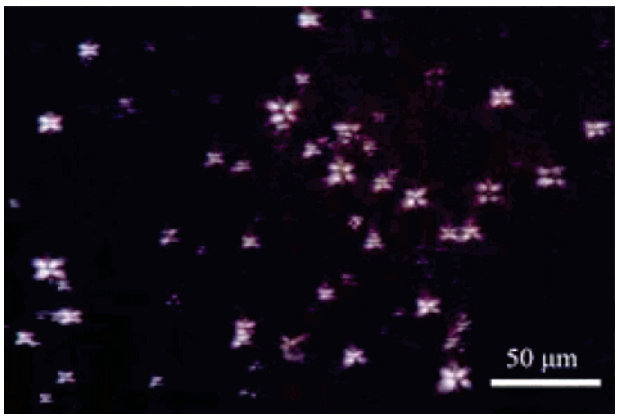

Figure 8. Polarized optical microscopy image of S-8, taken at 200 °C.

mesophase structure of MJLCPs, in contrast to reported conventional star SCLCPs. The amorphous state and Φ_N phase of linear PMPCS with moderate molecular weight develop to a

more ordered Φ_{HN} phase when they are linked together to form eight-arm star PMPCS.

For low molecular weight liquid crystals, it is common that the star-shaped molecules are liquid crystals while their arms are not,[53,54] but it is unusual for star LCPs. We suppose that the interesting properties of the eight-arm star PMPCS are due to the unique chain conformation of MJLCPs. As mentioned above, the jacketed effect of the rigid mesogenic side chains makes the conformation of whole polymer chain become semirigid, so supramolecular columnar phase is formed by parallel packing of the rodlike polymer chains, not by the alignment of mesogenic side groups. Thus, each arm of the star PMPCS can be looked as a huge mesogen. The linear PMPCS with high enough molecular weight are enantiotropic mesogens,[38] so enantiotropic liquid crystalline phase remains when these mesogens are linked together. Linear PMPCS with molecular weight higher than 0.70×10^4 g/mol but lower than 1.00×10^4 g/mol have decreasing rigidity compared to the high molecular weight ones, so they are virtual mesogens. When these virtual mesogens are "polymerized" to form eight-arm star polymers, an enantiotropic mesophase is achieved, as Percec and Keller described in their interpretation of molecular weight effect on the phase transitions of liquid crystalline polymers.[55] Therefore, the eight-arm star PMPCS requires fewer monomer units per arm to stabilize the liquid crystalline phase. On the other hand, the supramolecular columnar phase of the star PMPCS is formed by the parallel packing of cylinder-like arms, not by the alignment of mesogenic side groups. If we consider the initiator core as a sphere, its surface area is about 18 nm^2, so each polymer arm occupies an area of 2.3 nm^2. The area of the cross section of each column formed by PMPCS arm is about 2.4 nm^2. The area close to the surface of initiator core can be considered as the most confined environment to the arms. In this area, PMPCS columns have to pack densely; thus, the hexagonal symmetric packing model is favored.

Conclusion

Well-defined eight-arm star mesogen-jacketed liquid crystalline polymers with controlled molecular weight and low polydispersity have been prepared via ATRP of MPCS using OBPS as initiator. Radical coupling does not occur during the polymerization, even at high monomer conversion, as evidenced by gel permeation chromatography line equipped with a multiangle laser light scattering detector. The starlike macromolecule is demonstrated to have eight arms by comparing the molar mass of stars with those of their corresponding arms.

Combining 1D and 2D WAXD results with POM observations, molecular weight dependent phase behavior of the eight-arm star PMPCS samples has been investigated. When $M_{n,star}^{GPC}$ is lower than 4.48×10^4 g/mol ($M_{n,arm}^{GPC} = 0.74 \times 10^4$ g/mol), only amorphous state can be observed; when $M_{n,star}^{GPC}$ reaches or exceeds this value, Φ_{HN} phase develops. The amorphous state and Φ_N phase of the moderate molecular weight linear PMPCS develop to more ordered Φ_{HN} phase by linking them together to form eight-arm star polymers. The mesophase of the star MJLCPs is formed by the parallel packing of rodlike arms, so the starlike architecture of the macromolecules is found to affect the mesophase structure of MJLCPs, in contrast to reported conventional star SCLCPs.

Acknowledgment. The work described in this paper was supported by the National Natural Science Foundation of China (Grants 20634010 and 20574002), National ''973" Project (G2003CB615605), and the Science Research Fund of the Chinese Ministry of Education (Grant 104005).

References and Notes

(1) Ishizu, K.; Tusubaki, K.; Mori, A.; Uchida, S. *Prog. Polym. Sci.* **2003**, *28*, 27−54.
(2) Grest, G. S.; Fetters, L. J.; Huang, J. S.; Richter, D. In *Advances in Chemical Physics;* Wiley & Sons: New York, 1996; Vol. XCIV.
(3) Burchard, W. *Adv. Polym. Sci.* **1999**, *143*, 113−194.
(4) Hadjichristidis, N.; Pispas, S.; Pitsikalis, M.; Iatrou, H.; Vlahos, C. *Adv. Polym. Sci.* **1999**, *142*, 71−127.
(5) McLeish, T. C. B.; Milner, S. T. *Adv. Polym. Sci.* **1999**, *143*, 195−256.
(6) Reichert, V. R.; Mathias, L. J. *Macromolecules* **1994**, *27*, 7024−7029.
(7) Dong, C. M.; Qiu, K. Y.; Gu, Z. W.; Feng, X. D. *Macromolecules* **2001**, *34*, 4691−4696.
(8) Lin, W. J.; Chen, W. C.; Wu, W. C.; Niu, Y. H.; Jen, A. K. Y. *Macromolecules* **2004**, *37*, 2335−2341.
(9) Kasko, A. M.; Heintz, A. M.; Pugh, C. *Macromolecules* **1998**, *31*, 256−271.
(10) Kasko, A. M.; Pugh, C. *Macromolecules* **2004**, *37*, 4993−5001.
(11) Kasko, A. M.; Pugh, C. *Macromolecules* **2006**, *39*, 6800−6810.
(12) Kricheldorf, H. R.; Stukenbrock, T.; Friedrich, C. *J. Polym. Sci., Polym. Chem.* **1998**, *36*, 1387−1395.
(13) Yang, F.; Bai, Y.; Min, B. G.; Kumar, S.; Polk, M. B. *Polymer* **2003**, *44*, 3837−3846.
(14) Zhou, Q. F.; Li, H. M.; Feng, X. D. *Macromolecules* **1987**, *20*, 233−234.
(15) Zhou, Q. F.; Zhu, X. L.; Wen, Z. Q. *Macromolecules* **1989**, *22*, 491−493.
(16) Zhou, Q. F.; Wan, X. H.; Zhu, X. L.; Zhang, F.; Feng, X. D. *Mol. Cryst. Liq. Cryst.* **1993**, *231*, 107−117.
(17) Wan, X. H.; Zhang, F.; Wu, P.; Feng, X. D.; Zhou, Q. F. *Macromol. Symp.* **1995**, *96*, 207−218.
(18) Zhang, H.; Yu, Z.; Wan, X.; Zhou, Q. F.; Woo, E. M. *Polymer* **2002**, *43*, 2357−2361.
(19) Zhao, Y. F.; Fan, X. H.; Wan, X. H.; Chen, X. F.; Yi, Y.; Wang, L. S.; Dong, X.; Zhou, Q. F. *Macromolecules* **2006**, *39*, 948−956.
(20) Yi, Y.; Fan, X. H.; Wan, X. H.; Li, L.; Zhao, N.; Chen, X. F.; Xu, J.; Zhou, Q. F. *Macromolecules* **2004**, *37*, 7610−7618.
(21) Gao, L. C.; Pan, Q. W.; Yi, Y.; Fan, X. H.; Chen, X. F.; Zhou, Q. F. *J. Polym. Sci., Polym. Chem.* **2005**, *43*, 5935−5943.
(22) Gopalan, P.; Zhang, Y.; Li, X.; Wiesner, U.; Ober, C. K. *Macromolecules* **2003**, *36*, 3357−3364.
(23) Kennedy, J. P.; Jacob, S. *Acc. Chem. Res.* **1998**, *31*, 835−841.
(24) Wang, J. S.; Matyjaszewski, K. *J. Am. Chem. Soc.* **1995**, *117*, 5614.
(25) Angot, S.; Murthy, K. S.; Taton, D.; Gnanou, Y. *Macromolecules* **1998**, *31*, 7218−7225.
(26) Angot, S.; Murthy, K. S.; Taton, D.; Gnanou, Y. *Macromolecules* **2000**, *33*, 7261−7274.
(27) Ueda, J.; Kamigaito, M.; Sawamoto, M. *Macromolecules* **1998**, *31*, 6762−6768.
(28) Heise, A.; Hedrick, J. L.; Frank, C. W.; Miller, R. D. *J. Am. Chem. Soc.* **1999**, *121*, 8647−8648.
(29) Heise, A.; Hedrick, J. L.; Trollsas, M.; Miller, R. D.; Frank, C. W. *Macromolecules* **1999**, *32*, 231−234.
(30) Heise, A.; Nguyen, C.; Malek, R.; Hedrick, J. L.; Frank, C. W.; Miller, R. D. *Macromolecules* **2000**, *33*, 2346−2354.
(31) Heise, A.; Diamanti, S.; Hedrick, J. L.; Frank, C. W.; Miller, R. D. *Macromolecules* **2001**, *34*, 3798−3801.
(32) Costa, R. O. R.; Vasconcelos, W. L.; Tamaki, R.; Laine, R. M. *Macromolecules* **2001**, *34*, 5398−5407.
(33) Jankova, K.; Bednarek, M.; Hvilsted, S. *J. Polym. Sci., Polym. Chem.* **2005**, *43*, 3748−3759.
(34) Xue, L.; Agarwal, U. S.; Zhang, M.; Staal, B. B. P.; Muller, A. H. E.; Bailly, C. M. E.; Lemstra, P. J. *Macromolecules* **2005**, *38*, 2093−2100.
(35) Ohno, K.; Wong, B.; Haddleton, D. M. *J. Polym. Sci., Polym. Chem.* **2001**, *39*, 2206−2214.
(36) Matyjaszewski, K.; Miller, P. J.; Pyun, J.; Kickelbick, G.; Diamanti, S. *Macromolecules* **1999**, *32*, 6526−6535.
(37) Percec, V.; Barboiu, B.; Bera, T. K.; van der Sluis, M.; Grubbs, R. B.; Frechet, J. M. J. *J. Polym. Sci., Polym. Chem.* **2000**, *38*, 4776−4791.
(38) Ye, C.; Zhang, H. L.; Huang, Y.; Chen, E. Q.; Lu, Y. L.; Shen, D. Y.; Wan, X. H.; Shen, Z. H.; Cheng, S. Z. D.; Zhou, Q. F. *Macromolecules* **2004**, *37*, 7188−7196.
(39) Zhang, D.; Liu, Y. X.; Wan, X. H.; Zhou, Q. F. *Macromolecules* **1999**, *32*, 5183−5185.
(40) Yi, Y.; Wan, X. H.; Fan, X. H.; Dong, R.; Zhou, Q. F. *J. Polym. Sci., Polym. Chem.* **2003**, *41*, 1799−1806.

(41) Zhao, Y. F.; Fan, X. H.; Chen, X. F.; Wan, X. H.; Zhou, Q. F. *Polymer* **2005**, *46*, 5396−5405.
(42) Gopalan, P.; Ober, C. K. *Macromolecules* **2001**, *34*, 5120−5124.
(43) Waddon, A. J.; Coughlin, E. B. *Chem. Mater.* **2003**, *15*, 4555−4561.
(44) Bassindale, A. R.; Pourny, M.; Taylor, P. G.; Hursthouse, M. B.; Light, M. E. *Angew. Chem., Int. Ed.* **2003**, *42*, 3488−3490.
(45) Zheng, L.; Hong, S.; Cardoen, G.; Burgaz, E.; Gido, S. P.; Coughlin, B. *Macromolecules* **2004**, *37*, 8606−8611.
(46) Waddon, A. J.; Zheng, L.; Farris, R. J.; Coughlin, B. *Nano Lett.* **2002**, *2*, 1149−1155.
(47) Leu, C. M.; Reddy, G. M.; Wei, K. H.; Shu, C. F. *Chem. Mater.* **2003**, *15*, 2261−2265.
(48) Chou, C. H.; Hsu, S. L.; Dinakaran, k.; Chiu, M. Y.; Wei, K. H. *Macromolecules* **2005**, *38*, 745−751.
(49) Saez, I. M.; Goodby, J. W. *Liq. Cryst.* **1999**, *26*, 1101−1105.
(50) Saez, I. M.; Goodby, J. W. *J. Mater. Chem.* **2001**, *11*, 2845−2851.
(51) Saez, I. M.; Goodby, J. W.; Richardson, R. M. *Chem.—Eur. J.* **2001**, *7*, 2758−2764.
(52) Tang, H.; Zhu, Z. G.; Wan, X. H.; Chen, X. F.; Zhou, Q. F. *Macromolecules* **2006**, *39*, 6887−6897.
(53) Lattermann, G. *Liq. Cryst.* **1987**, *2*, 723−728.
(54) Lehmann, M.; Gearba, R. I.; Koch, M. H. J.; Ivanov, D. A. *Chem. Mater.* **2004**, *16*, 374−376.
(55) Percec, V.; Keller, A. *Macromolecules* **1990**, *23*, 4347−4350.

MA070207D